ERDA/JPL - 954605 - 77/2
Distribution Category UC-63

DEVELOPMENT OF LOW-COST, HIGH ENERGY-PER-UNIT-AREA SOLAR CELL MODULES

Quarterly Report No. 2

Gregory T. Jones

Sanjeev Chitre

June 1977

JPL CONTRACT NO. 954605

Sensor Technology, Incorporated
21012 Lassen Street
Chatsworth, California 91311

This work was performed for the Jet Propulsion Laboratory California Institute of Techology, under NASA Contract NAS7-100 for the U.S. Energy Research and Development Administration, Divison of Solar Energy.

The JPL Low-Cost Silicon Solar Array Project is funded by ERDA and forms part of the ERDA Photovoltaic Conversion Program to initiate a major effort toward the development of low-cost solar arrays.

ABSTRACT

Work on the development of low-cost, high energy-per-unit area solar cell modules was conducted during this quarter. This project covers the period from April 1st, 1977 through June 30th, 1977 and is part of a two phase program.

Hexagonal solar cell and module efficiencies, module packing ratio, and solar cell design calculations were made. The cell grid structure and interconnection pattern was designed. The module substrate which includes the aluminum pan, aluminum plate, and mounting brackets were designed and fabricated for the three modules to be used in Phase I of this contract program. The hexagon computer program was delivered, however, it was returned for rework and debugging to fulfill the program specifications. Experience was gained on laserscribing and hexagon cutting from a substitute computer program. It was demonstrated that the laserscribe can clearly cut through the p-n junction of the solar cell without causing excessive current leakage across the junction. Full hexagons and half hexagons can be cut by laser without causing excessive loss in photovoltaic energy conversion efficiency.

The solar cell surface macrostructure study and diffusion study continued during this quarter for Phase II of this program. It was demonstrated that surface macrostructures significantly

improve solar cell power output and photovoltaic energy conversion efficiency. Silicon wafer surface preparation and etching time, temperature and concentration was optimized relative to surface macrostructures that trap light efficiently. The spectral response of these cells showed superior light absorption over our commercial solar cell. A diffusion furnace temperature profile study indicates that with only a few modifications to our equipment, 400 silicon wafers per hour can be diffused.

A study to determine the optimum silicon ingot diameter to be utilized for modified hexagonal solar cells as a function of the relative silicon material costs, solar cell packaging costs, and solar cell module system costs was completed during this quarter. A method was presented for determining the optimum low-cost, high energy-per-unit-area solar cell module system.

TABLE OF CONTENTS

	Page
ABSTRACT	i
TABLE OF CONTENTS	iii
LIST OF FIGURES	v
LIST OF TABLES	vii
INTRODUCTION	1
TECHNICAL DISCUSSION - SECTION I	2
A. Hexagonal Solar Cell	
B. Hexagonal Solar Cell Nesting Efficiency	
C. Hexagonal Solar Cell Module Packing Ratio	
D. Hexagonal Solar Cell Module Fabrication	
1) Module Substrate	
2) Hexagonal Solar Cells and Interconnections	
3) Encapsulation Material	
E. Laserscribe	
TECHNICAL DISCUSSION - SECTION II	14
A. Surface Macrostructure	
B. Diffusion	
TECHNICAL DISCUSSION - SECTION III	21
A. Optimum Silicon Utilization in Modified Hexagonal Solar Cells	
B. Optimum Solar Cell Module System	
CONCLUSIONS	31

Page

RECOMMENDATIONS 32

NEW TECHNOLOGY 33

PROGRESS SUMMARY AND PROGRAM PLAN 34

APPENDIX. 37

A. Calculation of the Optimum Silicon Utilization in Modified Hexagonal Solar Cells.

B. List of Definitions

LIST OF FIGURES

Figure		Page
1	"Sensagon" hexagonal solar cell. . . .	3
2	Electrical performance curve of hexagonal solar cell.	4
3	Hexagonal solar cell module.	6
4	Schematic diagram of the interconnection pattern for the hexagonal solar cell module.	9
5	Electrical performance curves for the hexagonal solar cell and for the half hexagonal solar cell.	11
6	Quantronix Corporation's Laserscribe 603-2 and Sensor Technology's hexagonal solar cell module.	12
7	Electrical performance curve for Sensor Technology's hexagonal solar cell module.	13
8	SEM picture of silicon surface macro-structure etched by NaOH:water solution at 4000X.	15
9	Spectral response curves comparing Sensor Technology's commercial solar cell with RTV-615 encapsulant and surface macro-structure solar cell with RTV-615 encapsulant. The curves show that solar cells with surface macrostructure absorb more light than the commercial process solar cells.	17
10	Spectral response curves, normalized, comparing Sensor Technology's commercial solar cell with RTV-615 encapsulant and surface macrostructure solar cell with RTV 615 encapsulant. The curves show that the junction depth is the same for both solar cells.	18

Figure		Page
11	Variation in sheet resistivity along the length of the diffusion tube after 200 ninety millimeter diameter silicon wafers per half hour run diffusion.	20
12	Modified hexagon with unit radius scribed from a circular silicon wafer.	22
13	Relationship between the fractional utilization of the silicon wafer and modified hexagon for a varying normalized cylinderical silicon wafer radius and for varying costs, i.e. ¼, ½, 1, 1½, 2 and 3 times the unit silicon cost.	24
14	For a given hexagon center to point radius, the curves show the cost radii for a cylinderical silicon ingot versus the silicon plus packaging incremental costs. The minimum radius is marked on each curve.	25
15	For a given hexagon center to point radius the curve shows the minimum cost radius for a cylinderical silicon ingot as a function of the silicon cost to solar cell packaging cost.	26
16	Power of modified hexagon per unit area relative to the full normalized hexagon.	29
17	Development of Low-Cost, High Energy-Per-Unit-Area Solar Cell Modules; Phase I and Phase II Program Plan.	36
18	Section of modified hexagon illustrating silicon area (t x u) loss and hexagon area (u v w) loss.	39

LIST OF TABLES

Table		Page
1	Calculated results for determining the fractional utilization of silicon.	41
2	Calculated results for determining the fractional utilization of the modified hexagon.	43
3	Calculated results for determining the fractional utilization of silicon for various costs, i.e. ¼, ½, 1, 1½, 2, 3 times the unit cost of silicon.	45
4	Calculated results for determining the incremental cost of the silicon material thrown away plus the solar cell packaging for normalized silicon ingot radii between .866 and 1.000. Included is the minimum cost radii read from the curves in Figure 15.	47

INTRODUCTION

Development of low-cost, high energy-per-unit-area solar cell modules is the overall goal of this program. Effort was directed during this quarter toward achieving the goals of Phase I. Hexagonal solar cells were cut using the laserscribe and the Phase I hexagonal solar cell module was designed and the first of three modules was constructed. The diffusion studies related to the 400 wafer per hour capability were completed along with the studies on the modified hexagons which show how to achieve maximum economy for the development of low-cost, high-energy-per-unit-area solar cell modules. Studies continued on the diffusion processes and surface macrostructure processes.

During the third quarter effort will be directed toward completing the program. This will include surface macrostructure studies, diffusion studies and cost analysis studies. Spin on equipment is being procured and studies will be made. The remaining modules for Phase I and the modules for Phase II will be completed.

Portions of this quarterly report were contributed by Paul A. Dennis and Irwin Rubin.

TECHNICAL DISCUSSION - SECTION I

A. Hexagonal Solar Cell

A hexagonal solar cell with a point to point diameter of 3.500 inches and a side to side diameter of 3.031 inches is used in Phase I of this program. The surface area of the hexagonal solar cell is 7.956 square inches. The production process is the same as used for Sensor Technology's commercial solar cells with the exception of scribing the solar cell with the laser-scribe. The grid pattern consists of three main grid lines in a "y" arrangement 120^{o} with respect to each other and has hexagonal fine grid lines symmetrical about the center of the solar cell. The solar cell is adaptable to being cut into halves and arranged in a unique solar cell interconnection pattern. The "Sensagon" hexagonal solar cell is shown in Figure 1. The electrical performance of the hexagonal solar cell is shown in Figure 2. The average maximum power is .45 watts with a photovoltaic energy conversion efficiency of 9.4% under tungsten light at $28^{o}C$ and at 100 mw/cm^2.

Sensor Technology's commercial process is used on 2.15 inch diameter solar cells with a resulting photovoltaic energy conversion efficiency of 11% at $28^{o}C$ and at 100 mw/cm^2. Results from this program show that 3.54 inch diameter silicon solar cells have approximately 1.5% lower efficiencies with the identical process used on the smaller 2.15 inch diameter solar cells. Since Phase II of this program requires an entirely different solar cell process, future efforts will be concentrated on it rather than modifying the Phase I process.

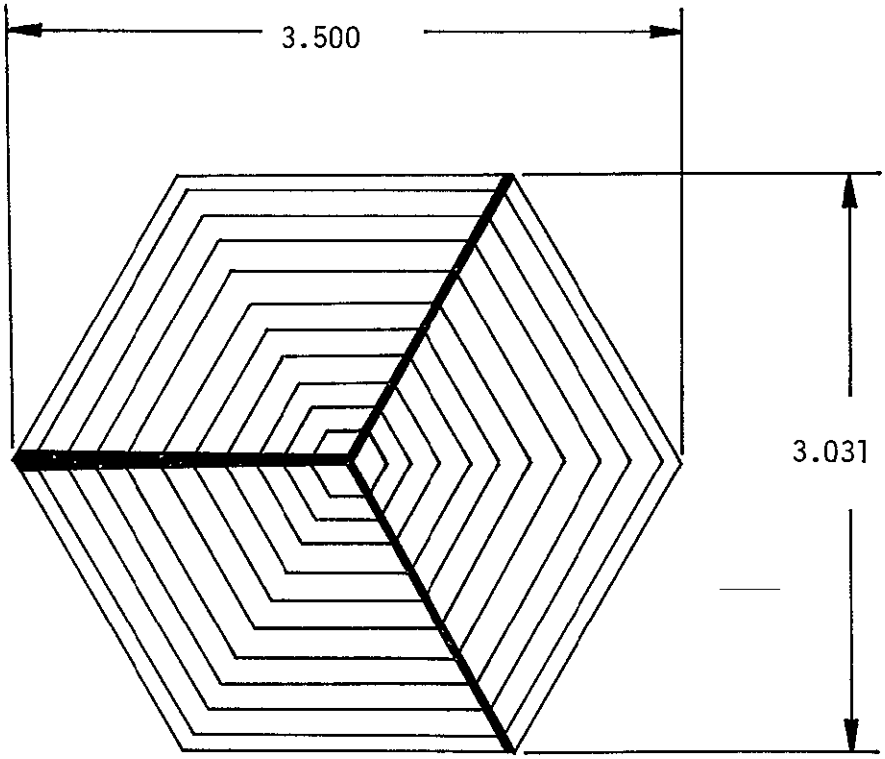

Figure 1. "Sensagon" hexagonal solar cell.

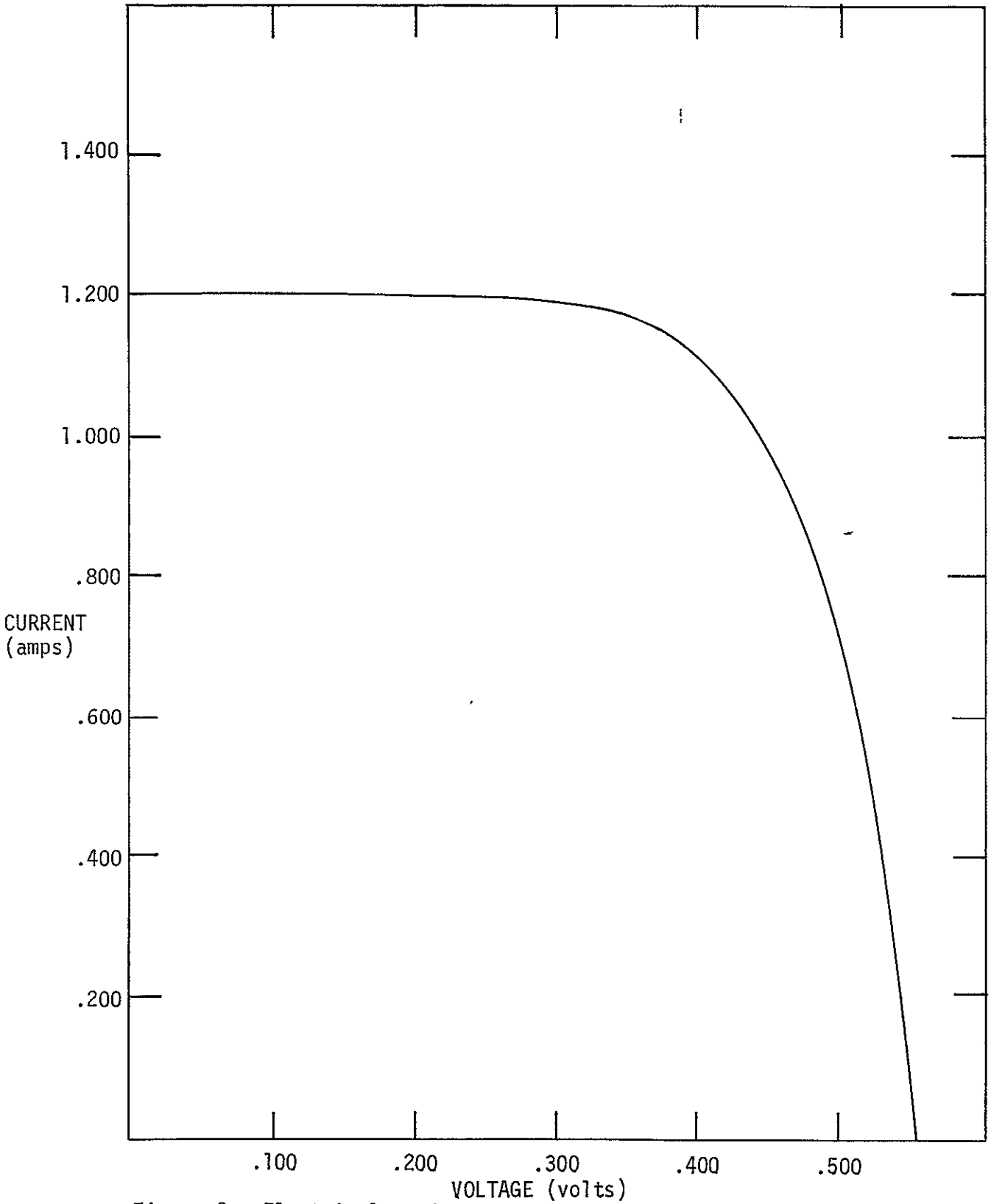

Figure 2. Electrical performance curve of hexagonal solar cell under tungsten light at 28°C and at 100 mw/cm^2.

B. Hexagonal Solar Cell Nesting Efficiency

The hexagonal solar cell nesting efficiency is defined as the ratio of the total hexagonal solar cell surface area to the nesting surface area that contains the solar cells which includes the total solar cell surface area plus the solar cell spacing area. The nesting area contains 28 hexagonal solar cells which are spaced 0.050 inches apart. Refer to Figure 3 top view for the following listed dimensions and calculations:

Solar cell nesting length	=	21.67 inches
Solar cell nesting width	=	10.77 inches
Nesting surface area	=	233.39 in^2
Total solar cell surface area	=	222.77 in^2
Solar cell spacing area	=	10.62 in^2
Solar cell nesting efficiency	=	95.5%

C. Hexagonal Solar Cell Module Packing Ratio

The hexagonal solar cell module packing ratio (or efficiency) is defined as the ratio of the total hexagonal solar cell surface area to the total solar cell module surface area. The module contains 28 hexagonal solar cells as shown in Figure 3, top view.

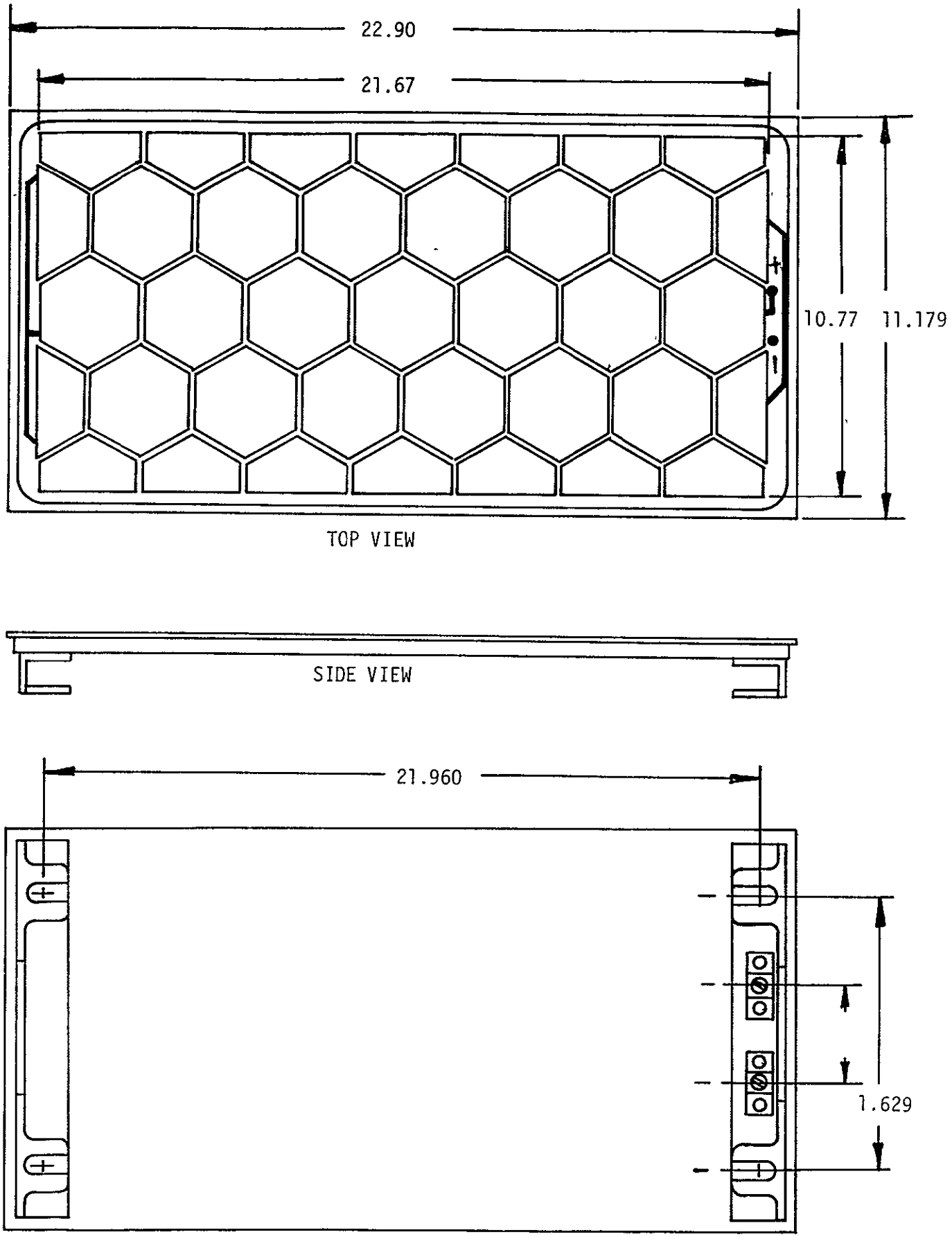

Figure 3. Hexagonal solar cell module. Shown are the front view, back view and side view of the module including the aluminum substrate pan, terminals, terminal connections, mounting brackets, and arrangement of the solar cells.

Module length	=	22.90 inches
Module width	=	11.179 inches
Module surface area	=	256.00 in^2
Total solar cell surface area	=	222.77 in^2
Module packing ratio	=	87%

D. Hexagonal Solar Cell Module Fabrication

1) Module Substrate

Sensor Technology is utilizing a JPL approved module substrate that we presently have in stock for the three modules to be produced in Phase I. The module substrate is a stampled aluminum pan. Minor additions to the stamped aluminum pan to meet our specific requirements are shown in Figure 3, bottom view, and are listed as follows:

a) Additional aluminum sheet to cover the top of the aluminum pan. It covers the terminal holes and mounting spacer holes that are presently on the pan. The aluminum sheet and pan are spot welded together.

b) Aluminum mounting brackets are spot welded to the aluminum substrate pan.

c) Two single wire terminals are utilized.

2) Hexagonal Solar Cells and Interconnections

Twenty eight solar cells will be utilized in the module. They consist of 19 hexagons and 18 half hexagons. Of the eighteen half hexagons, fourteen are cut side to side and four are cut point to point. Nine series connected half hexagons are paired in parallel with nine other half hexagons which are connected in series with eighteen hexagonal solar cells. The interconnection pattern is schematically shown in Figure 4.

3) Encapsulation Material

The encapsulation material used is General Electric RTV-615.

E. Laserscribe

The laserscribe was delivered and installed during the first two weeks in April. Minor equipment problems were debugged, an experience on laserscribing was gained during the second two weeks in April. X-Y scribing, depth of cut versus velocity of the laserscribe, and pulse rate of the light was studied.

The hexagon computer program was delivered the last day in May, but it was found to require additional debugging and program development to meet the required specifications. The entire printed circuit board was returned to Quantronix Corporation.

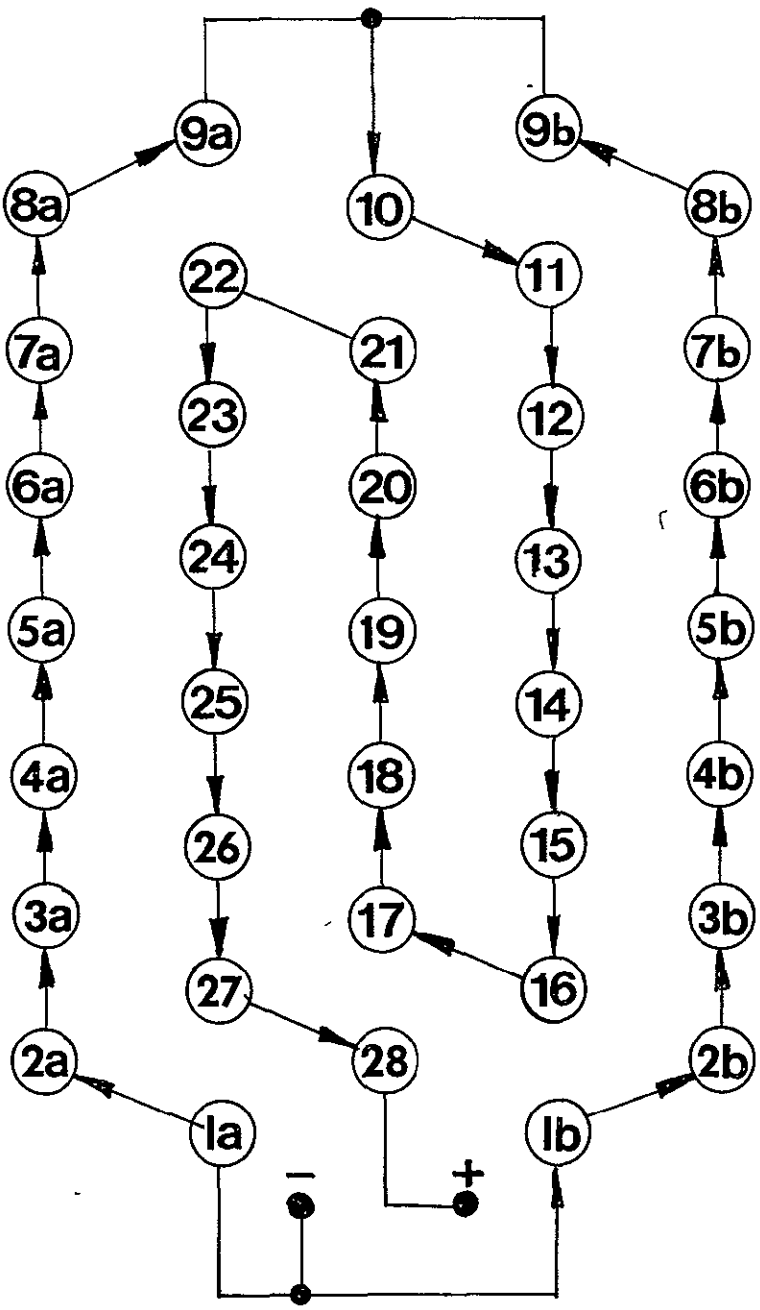

Figure 4. Schematic diagram of the interconnection pattern for the hexagonal solar cell module.

Experience was gained on laserscribing and hexagon cutting from a substitute computer program. It was demonstrated that the laserscribe can clearly cut through the p-n junction of the solar cell without causing excessive current leakage across the junction. Full hexagons and half hexagons can be cut by laser without causing excessive loss in photovoltaic energy conversion efficiency. These results are shown by the electrical performance in Figure 5 for a full hexagon and for the hexagon cut in half. The half hexagon has half the short circuit current of the full hexagon and the power point voltage is the same for both.

Quantronix Corporation's laserscribe 603-2 and Sensor Technology's first hexagonal solar cell module is shown in Figure 6. The electrical performance curve for the hexagonal solar cell module is shown in Figure 7. It produces 11.8 watts of power at $28^{o}C$ and at 100 mw/cm^2 under Xenon solar simulator.

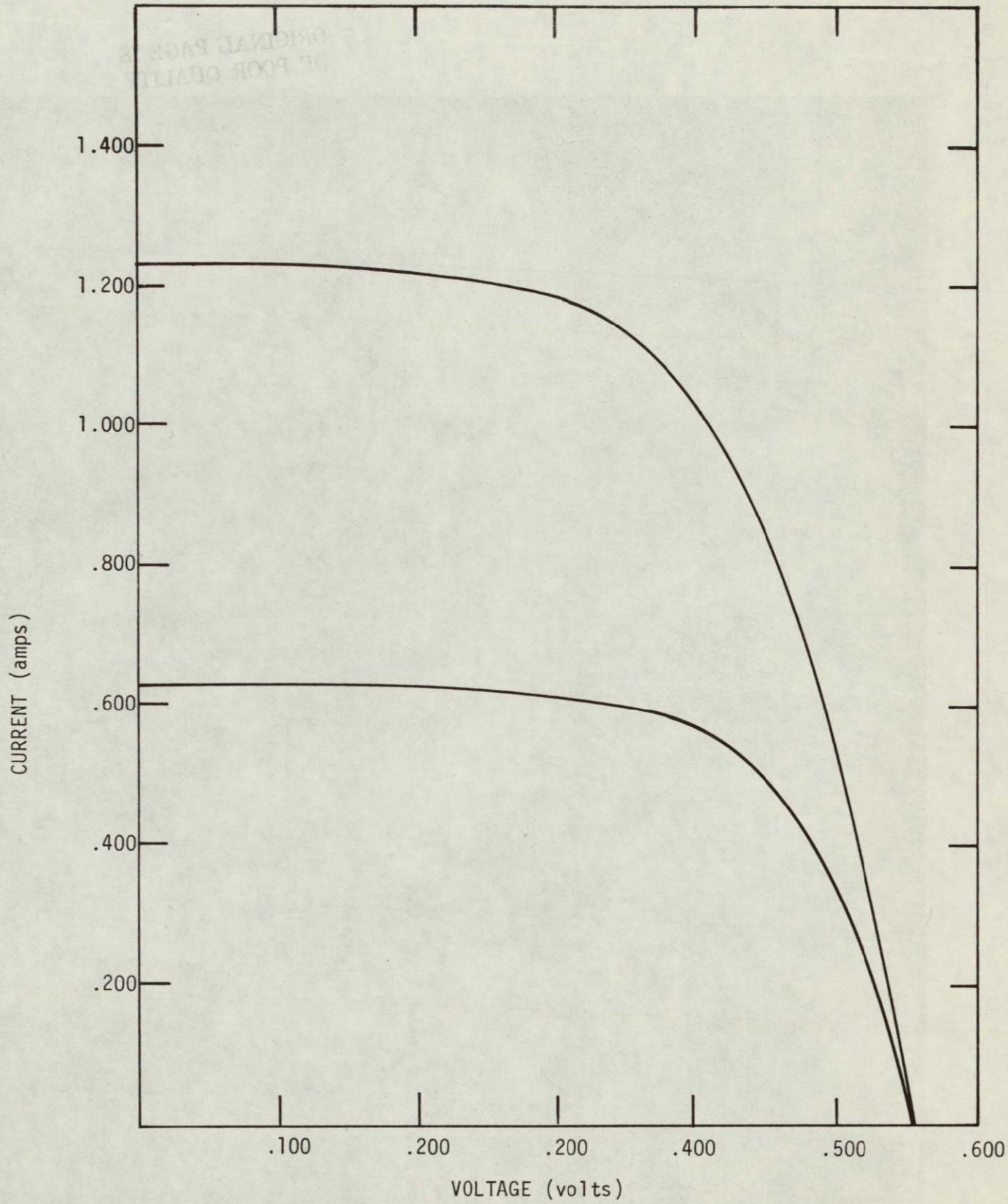

Figure 5. Electrical performance curves for a hexagonal solar cell half and for hexagonal solar cell. These solar cells have no A.R. coating and were tested at 28°C and at 100 mw/cm^2.

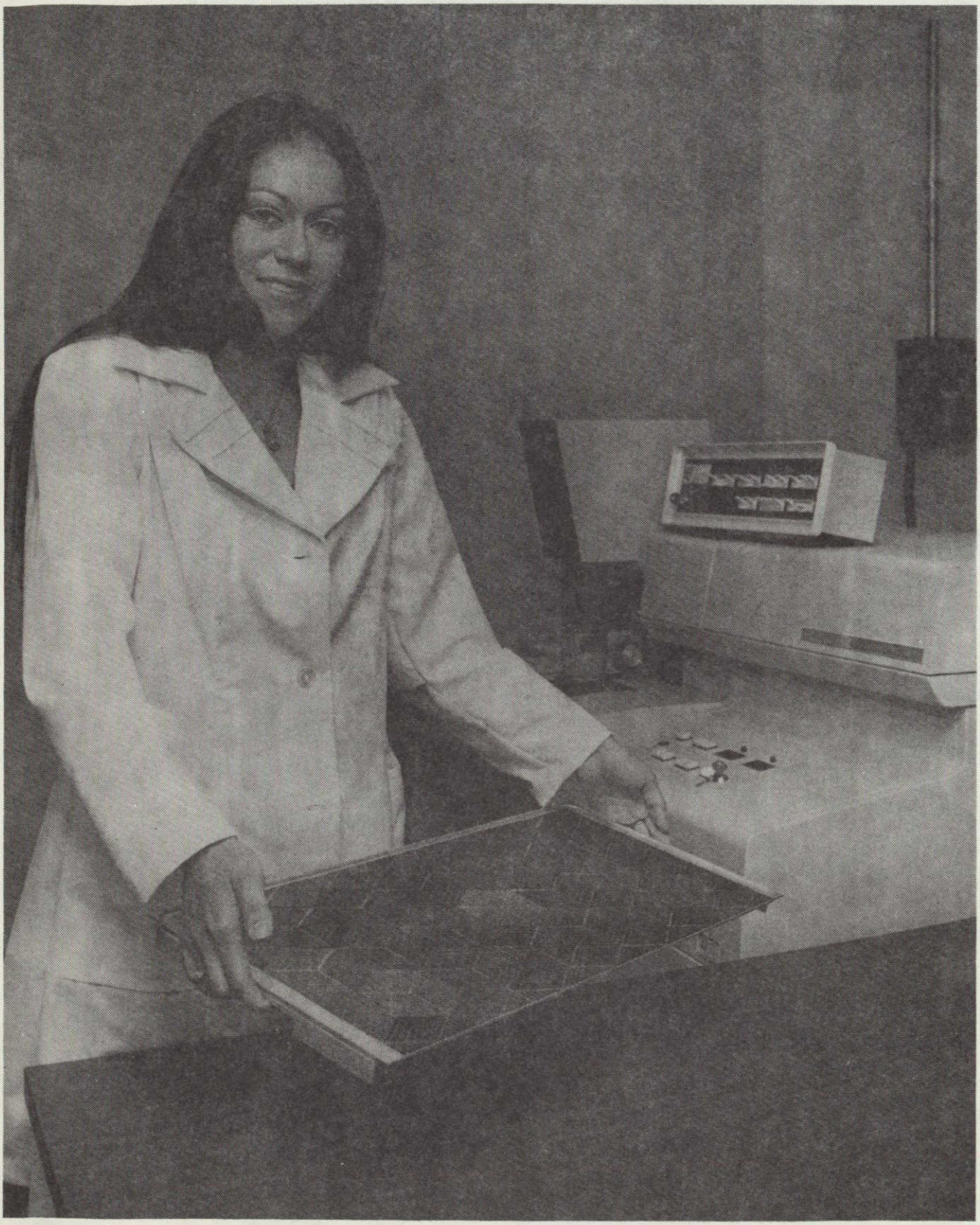

Figure 6. Quantronix Corporation's Laserscribe 603-2 and Sensor Technology's hexagonal solar cell module.

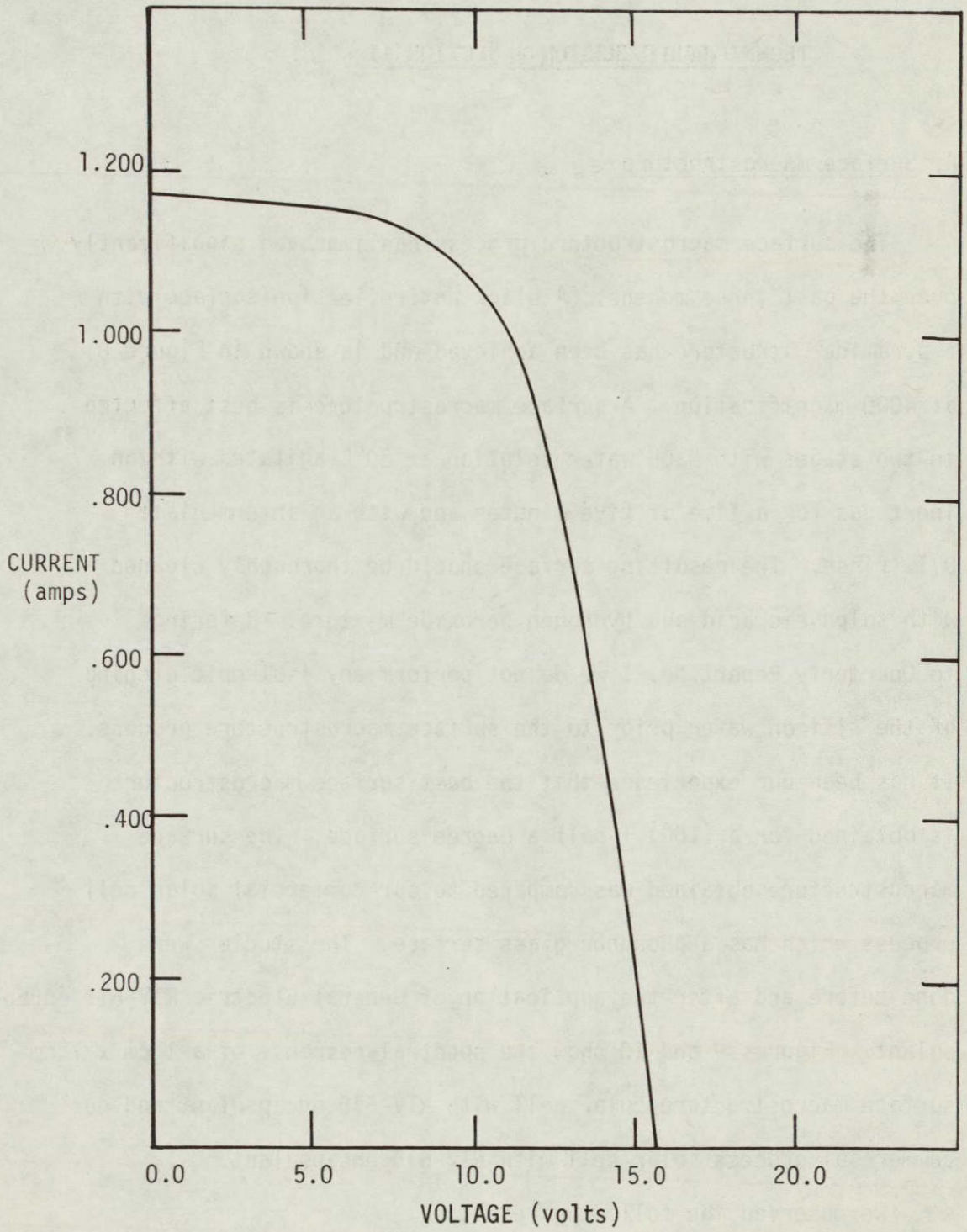

Figure 7. Electrical performance curve for Sensor Technology's hexagonal solar cell module under Xenon light at 28°C and at 100 mw/cm^2.

TECHNICAL DISCUSSION - SECTION II

A. Surface Macrostructure

The surface macrostructure process has improved significantly over the past three months. A black antireflection surface with a pyramidal structure has been achieved and is shown in Figure 8 at 4000 magnification. A surface macrostructure is best effected in two stages with NaOH water solution at 80°C agitated with an inert gas for a time of five minutes and with an intermediate D.I. rinse. The resulting surface should be thoroughly cleaned with sulphuric acid and hydrogen peroxide mixture. Refering to Quarterly Report No. 1 we do not perform any isotropic etching of the silicon wafer prior to the surface macrostructure process. It has been our experience that the best surface macrostructure is obtained for a (100) $\pm$ half a degree surface. The surface macrostructure obtained was compared to our commercial solar cell process which has a phosphor glass surface. The studies were done before and after the application of General Electric RTV-615 encapsulant. Figures 9 and 10 show the spectral response of a 1 cm x 1 cm surface macrostructure solar cell with RTV-615 encapsulant and our commercial process solar cell with RTV-615 encapsulant.

We observed the following results:

1. The absolute power output is higher for a solar cell with surface macrostructure than for our commercial solar cell because the former absorbs more incident radiation as shown in Figure 9.

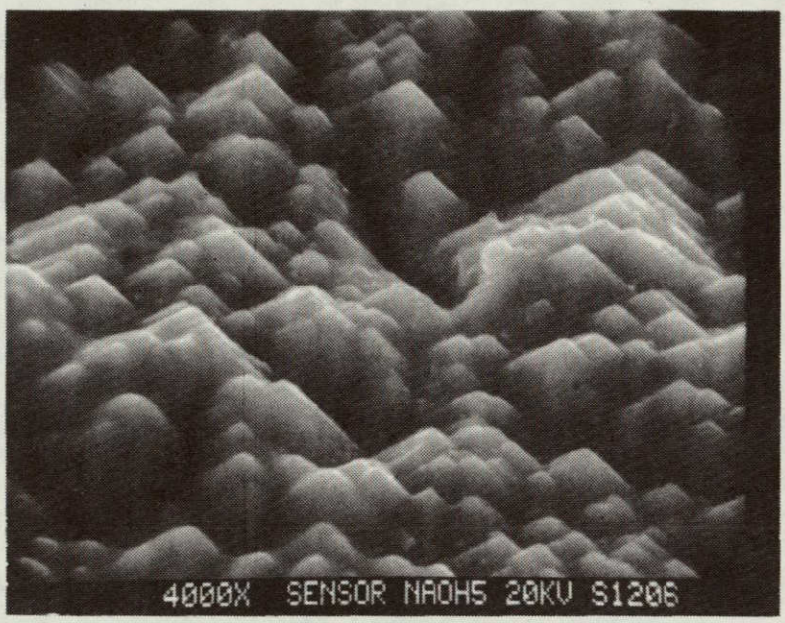

Figure 8. Sensor Technology's texturized solar cell 4000X

2. The spectral response is similar with and without RTV-615 encapsulant for solar cells with a surface macrostructure and for our commercial process solar cells. This is shown by the normalized spectral response curves in Figure 10.

3. For solar cells with the same p-n junction depth, the solar cells with surface macrostructure absorb more light in the lower wavelength and match the solar spectrum better than the commercial process solar cell as shown in Figure 9.

B. Diffusion

Experiments were carried out to diffuse 200 ninety millimeter silicon wafers in a half hour diffusion cycle. Diffusion boats of eighteen inches in length were designed and fabricated to accomodate 100 wafers per boat. Two such diffusion boats were introduced into a furnace with a 38 inch temperature flat zone of $900^{o}C \pm 5^{o}C$. The two diffusion boats were designed to allow for thermal stress and for convenience of loading and unloading. The diffusion was performed at approximately $900^{o}C \pm 5^{o}C$ in a 5.3/4 inch diameter tube six feet in length. The gas flow was adjusted for uniformity. The sheet resistivity was measured on a left, right and center wafers in each of ten rows. Each silicon wafer was measured at five surface points. A plot of the average sheet resistivity over the silicon wafer surface was

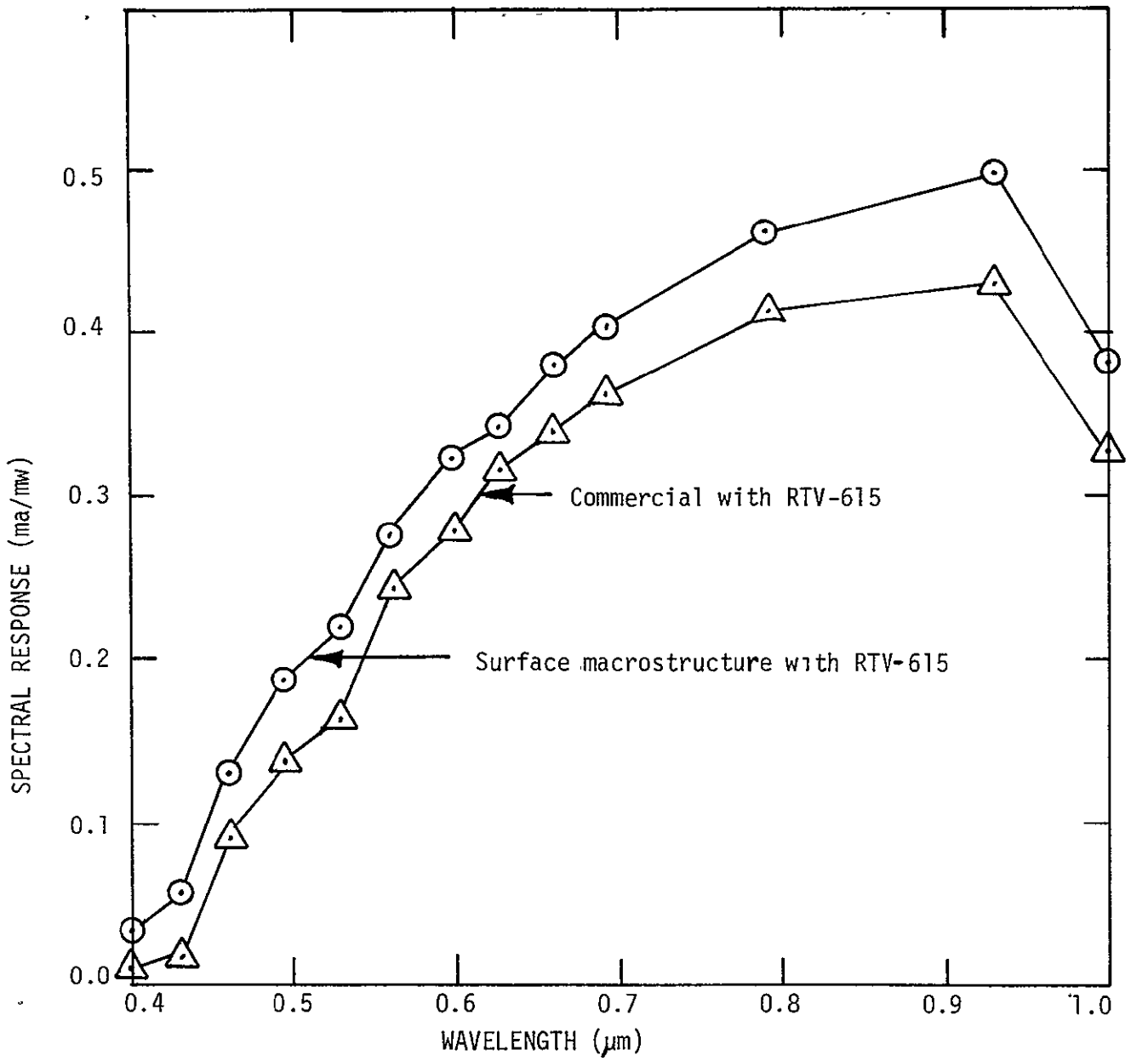

Figure 9. Spectral response curves comparing Sensor Technology's commercial solar cell with RTV-615 encapsulant and surface macrostructure solar cellwith RTV-615 encapsulant. The curves show that solar cells with surface macrostructure absorb more light than commercial process solar cells.

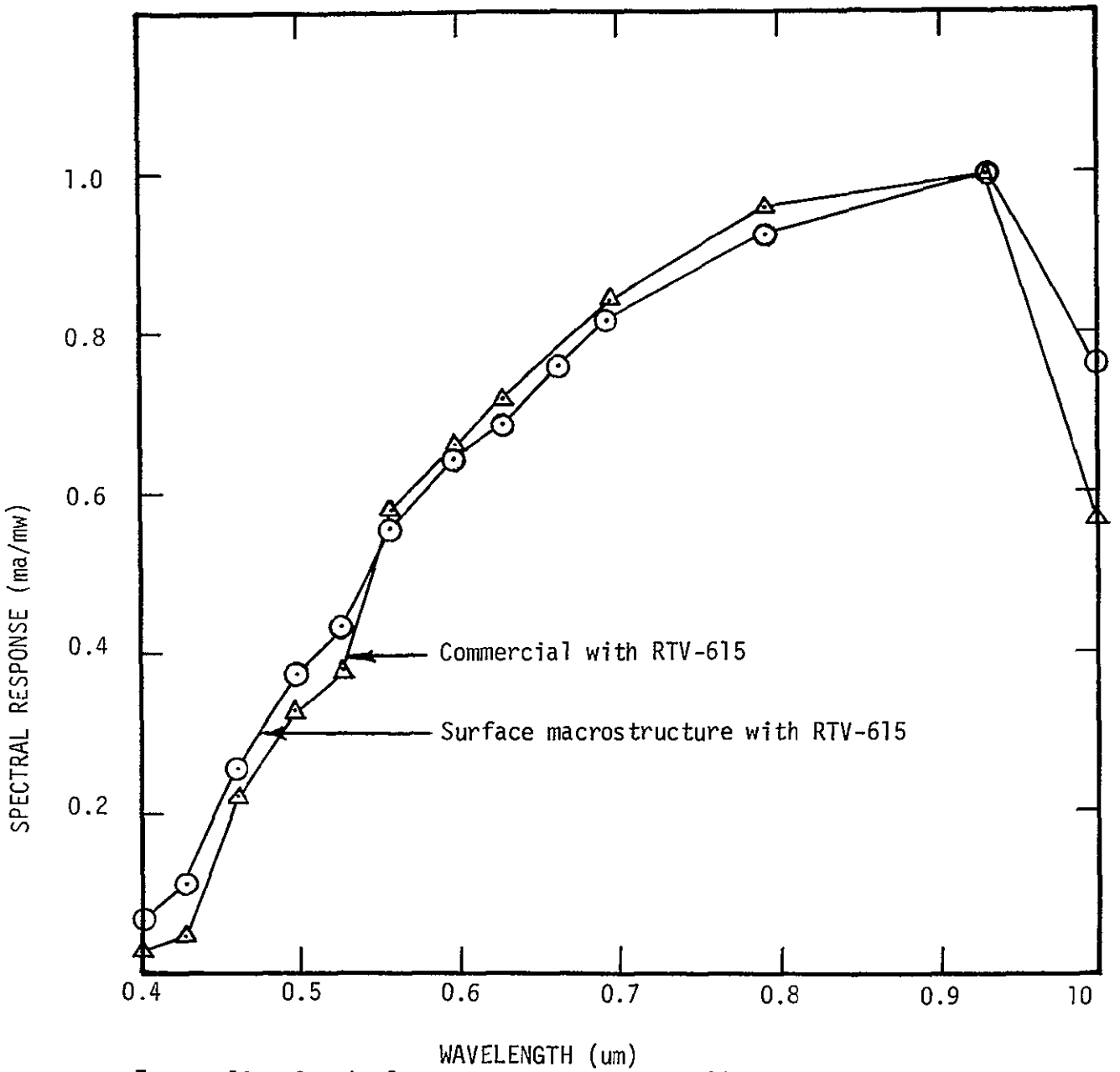

Figure 10. Spectral response curves, normalized comparing Sensor Technology's commercial solar cell with RTV 615, encapsulant and surface macrostructure solar cell with RTV 615 encapsulant. The curves show that the junction depth is the same for both solar cells.

made for the left, right and center wafers in each row which is shown in Figure 11. Spots of $POCl_3$ were visible on the silicon wafers due to the spitting effect.

The spitting effect was considerably reduced by the introduction of a buffered mixture. This mixture is introduced between the diffuser and the automatic gas flow meter panel. This buffer helps to thoroughly mix the gases prior to entering the diffuser and to remove traces of $POCl_3$ liquid drops which are carried by the gases. The variations in resistivity obtained with such a buffer with a modified usable temperature zone of $900^{o}C \pm 5^{o}C$ is shown in Figure 11.

It can be concluded that 400 ninety millimeter silicon wafers per hour can be diffused in a 38 inch flat zone furnace with the use of a buffered mixture to obtain a uniform sheet resistivity within 20%. This diffusion process allows one to process solar cells in large quantities with a 10% variation in photovoltaic energy conversion efficiency.

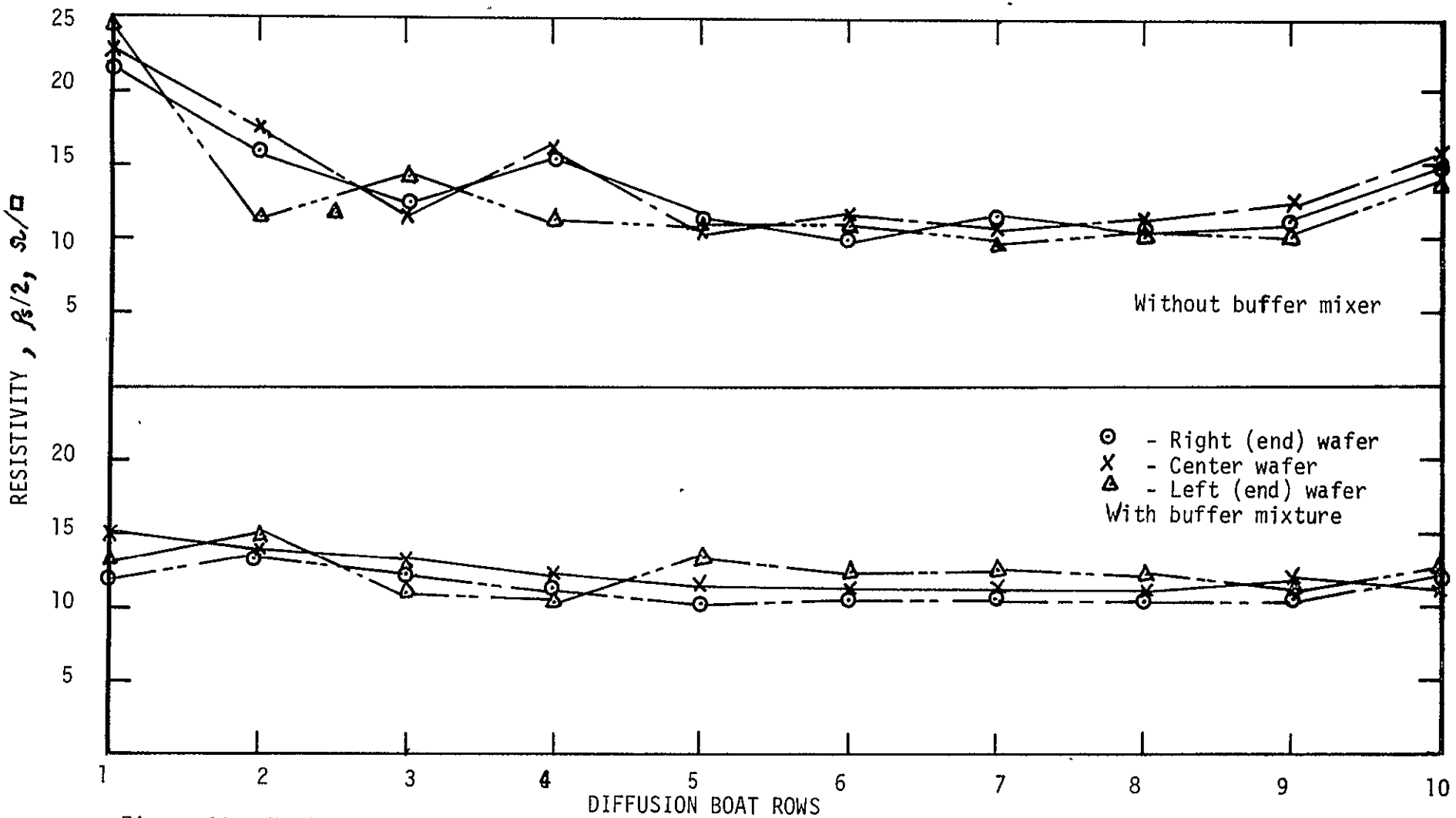

Figure 11. Variation in sheet resistivity along the length of the diffusion tube after 200 ninety millimeter diameter silicon wafers per half hour run diffusion.

TECHNICAL DISCUSSION - SECTION III

A. Optimum Silicon Utilization in Modified Hexagonal Solar Cells

This study determines the optimum silicon ingot diameter to be utilized for modified hexagonal solar cells as a function of the relative silicon material costs, solar cell packaging costs, and solar cell module system costs.

Figure 12 illustrates the relationship between the amount of silicon material lost and the amount of solar cell packaging material required when the modified hexagon is cut from the circular silicon wafer. For a hexagon with a fixed center to point radius equal to unity and with the cost of the silicon per unit area and the cost of the solar cell packaging material per unit area assumed to be equal, and at unit cost the following boundary conditions exist: At a radius of .866, one has an inscribed circular silicon wafer with respect to the full hexagon where 100% of the silicon is utilized, and 90.7% of the hexagon is used. At a radius of 1.000 one has a circumscribed silicon wafer with respect to the full hexagon where 82.7% of the silicon is utilized and 100% of the hexagon is used. For a given radius between .866 and 1.000, the fractional utilization of silicon material area to a full circular silicon wafer area can be calculated, and the fractional utilization of the modified hexagon area to the full hexagon area can be calculated.*

* Sample calculations are shown in Appendix A.

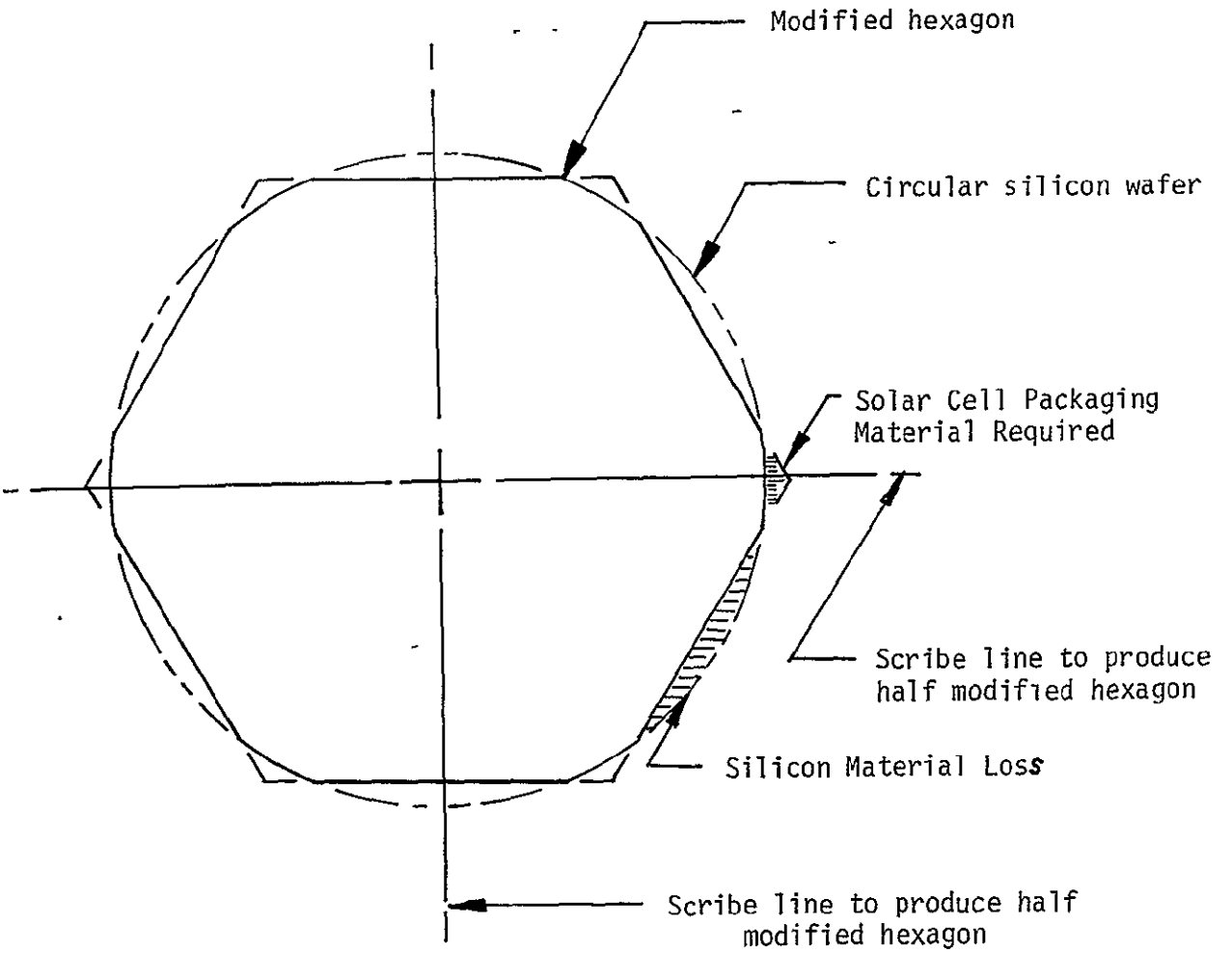

Figure 12. Modified hexagon with unit radius scribed from a circular silicon wafer.

The relationship between the fractional utilization of the silicon wafer and the fractional utilization of the modifed hexagon for a varying normalized cylinderical silicon wafer radius and for varying costs, i.e. for ¼, ½, 1, 1½, 2 and 3 times the unit silicon cost, is shown in Figure 13. The silicon cost curves were generated by weighting the silicon unit cost curve. The point of intersection of the curve in Figure 13 is a point where the fractional utilization of the silicon and modified hexagon is the same. However, the point of intersection is not an optimum point for utilization when costs are considered.

An incremental cost analysis can be made from the curves shown in Figure 13. The incremental cost is the sum of the silicon material costs thrown away plus the solar cell packaging costs for the wafer. The solar cell packaging costs include the material and labor costs of the module substrate and encapsulant required by the solar cell nesting area. The incremental costs for each curve in Figure 13 is shown in Figure 14. For a given hexagon center to point radius, the curves show the cost radii for a cylinderical silicon ingot versus the silicon plus packaging incremental costs. The minimum cost radius on each of these curves are plotted in Figure 15. Thus, for a given center to point radius the curve in Figure 15 shows the minimum cost radius for a cylinderical silicon ingot as a function of the silicon cost to solar cell packaging cost for a modified hexagon.

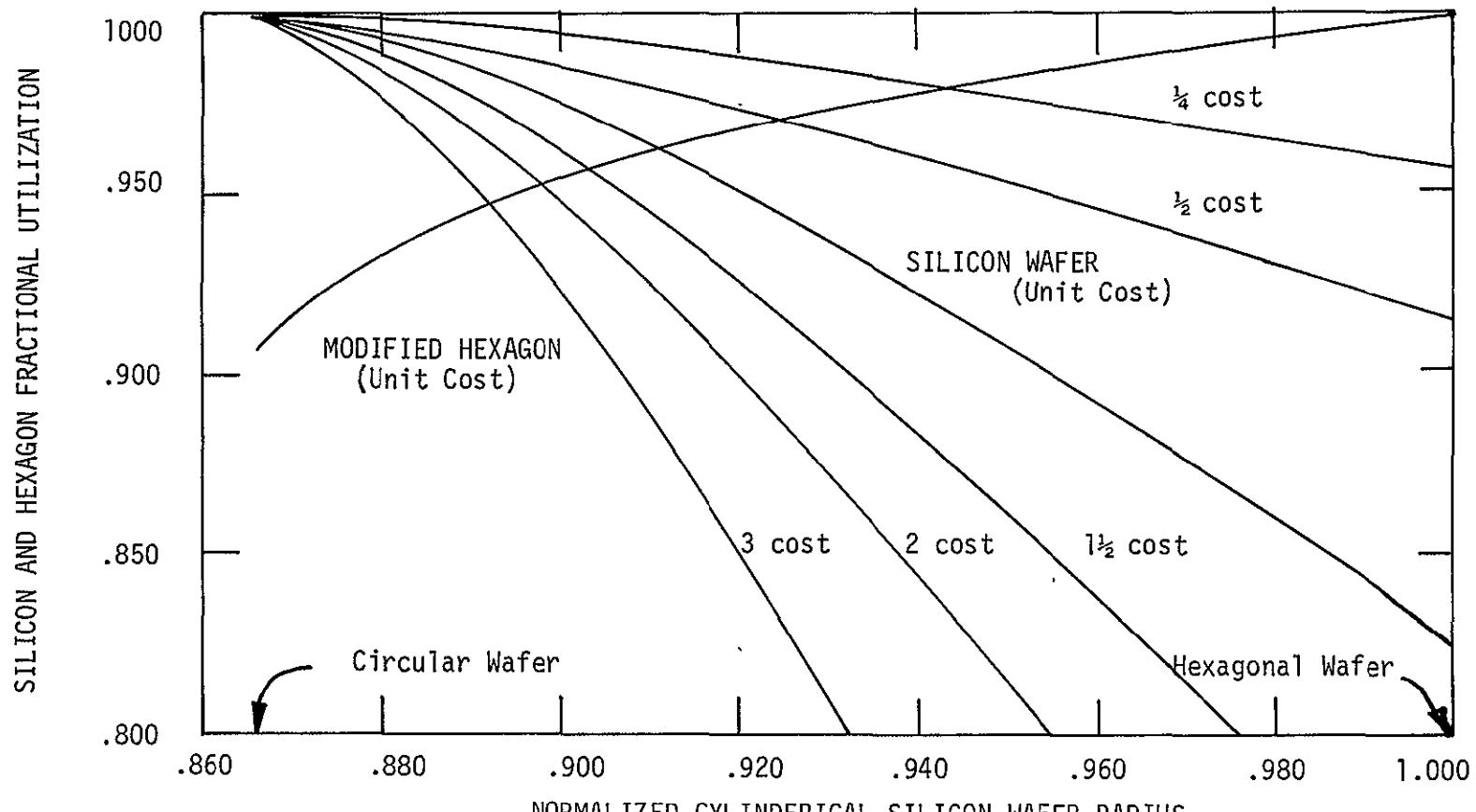

Figure 13. Relationship between the fractional utilization of the silicon wafer and modified hexagon for a varying normalized cylinderical silicon wafer radius and for varying costs, i.e. ¼, ½, 1, 1½, 2 and 3 times the unit silicon cost.

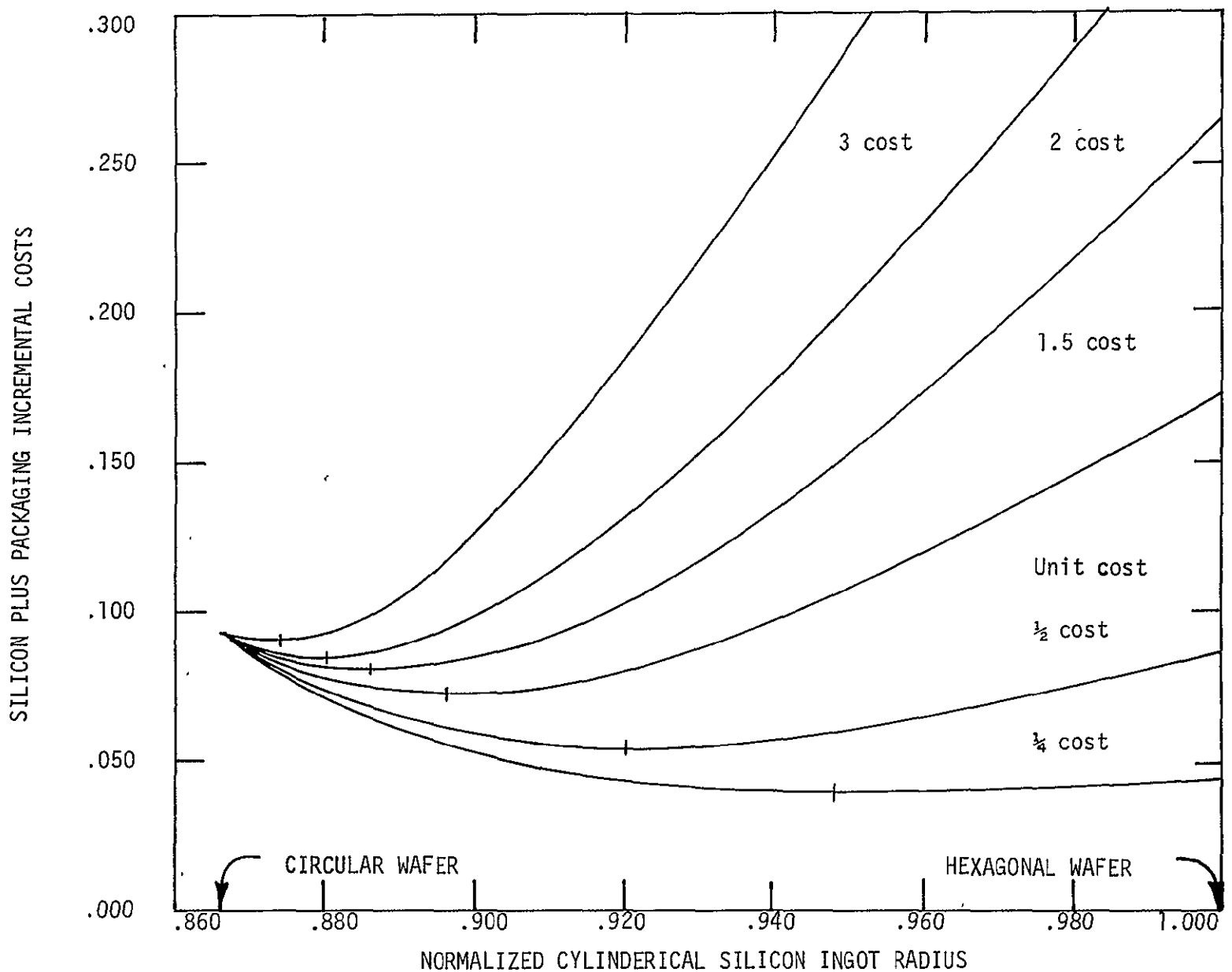

Figure 14 For a given hexagon center to point radius the curves show the cost radii for a cylinderical silicon ingot versus the silicon plus packaging incremental cost The minimum cost radius is marked on each curve.

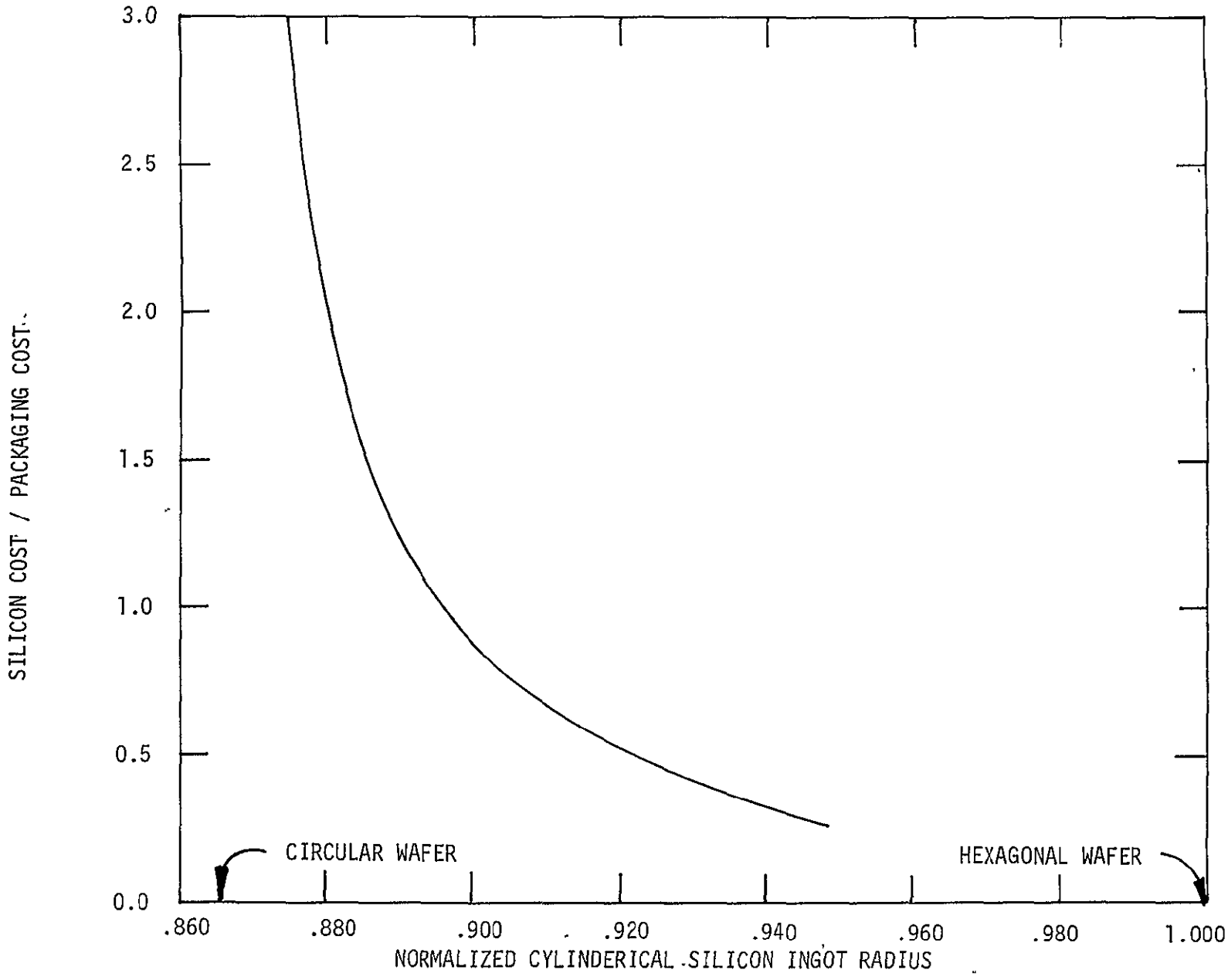

Figure 15. For a given hexagon center to point radius the curve shows the minimum cost radius for a cylinderical silicon ingot as a function of the silicon cost to solar cell packaging cost.

B. Optimum Solar Cell Module Systems

The optimum solar cell module system is determined by its application requirements. For applications that require maximum power per unit surface area one should use the full hexagonal solar cell module. Figure 16 shows the power of the modified hexagon per unit area relative to the full normalized hexagon. It is taken from the modified hexagon curve shown in Figure 13. It clearly shows that the full hexagon produces the maximum power per unit surface area.

Applications that require cost optimization should use a modified hexagonal solar cell module or related module where the ratio of silicon cost to solar cell packaging cost is a minimum as shown in Figure 15. The silicon cost is for the silicon wafer material. The solar cell packaging cost is the material and labor cost for the module substrate and encapsulant required by the solar cell nesting area.

Cost optimization should include the solar cell module system costs. The solar cell module system costs are the material and labor costs for the solar cell module, mounting frame, module interconnections and land area. It includes all fees and general expenses incurred in constructing the system.

An example that illustrates cost optimization for solar cell modules is presented as follows:

1. The spacial geometry of a given module substrate requires 3.54 inches (90 mm) point to point diameter hexagonal solar cells.

2. The present estimated ratio of silicon cost to solar cell packaging cost for mass production is 2.25.

3. The optimum silicon ingot diameter is determined from Figure 15. The normalized silicon ingot diameter for a silcion cost to solar cell packaging cost ratio of 2.25 is .878.

4. A hexagon with point to point diameter equal to 3.54 inches (90 mm) would require a silicon ingot grown to (.878) (3.54) = 3.11 inches (78.95 mm) in diameter for optimum silicon utilization in modified hexagonal solar cells.

5. For present solar cell module system costs the ratio of silicon cost to packaging cost for mass production is assumed to be 1.5.

6. The optimum silicon ingot diameter is determined from Figure 15. The normalized silicon ingot diameter for a silicon cost to packaging cost ratio of 1.5 is .886.

7. A hexagon with point to point diameter equal to 3.54 inches (90 mm) would require a silicon ingot grown to (.886) (3.54) = 3.14 inches (79.76 mm) in diameter for an optimum solar cell module system.

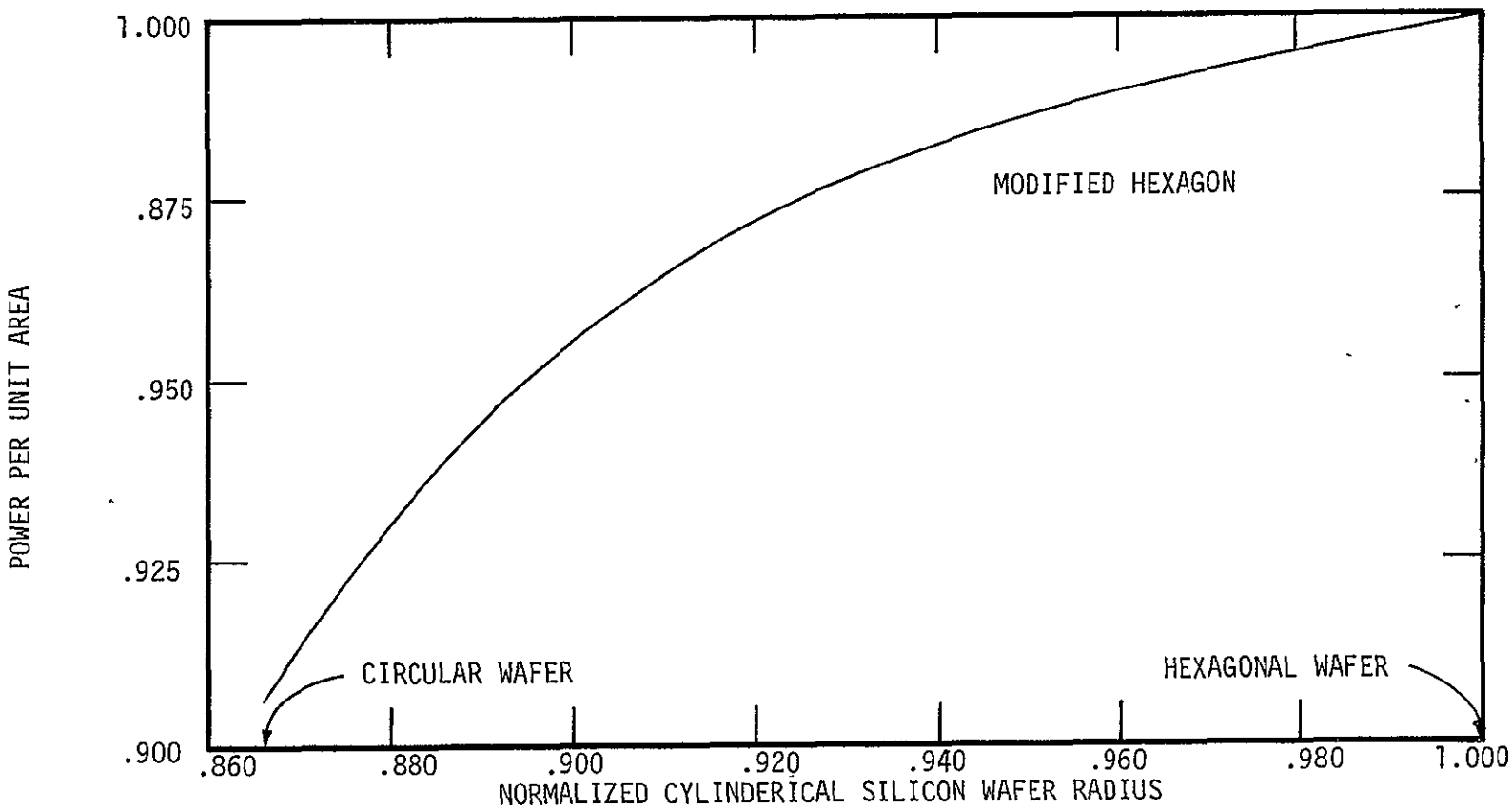

Figure 16. Power of Modified Hexagon per unit area relation to the full normalized hexagon.

JPL Contract 954605 for the Development of Low-Cost High Energy-Per-Unit-Area Solar Cell Modules utilizes 3.5 inch (88.9 mm) diameter hexagonal solar cells cut from 3.54 inch (90 mm) diameter circular silicon wafers. The diameter of the hexagons was chosen to suit the geometry of the module substrate. The contract goals are to achieve maximum power per-unit area. This is being done with the use of full hexagonal solar cells.

CONCLUSIONS

This program for the development of low-cost, high energy-per-unit-area solar cell modules has led to a number of conclusions. A laser can clearly cut through a p-n junction of the solar cell without causing excessive current leakage across the junction. Full hexagons and half hexagons can be cut by laser without causing excessive loss in photovoltaic energy conversion efficiency. An 87% solar cell packing ratio can be achieved with the use of full hexagons and half hexagons. Solar Cell surface macrostructures significantly improve solar cell power output and photovoltaic energy conversion efficiency. The spectral response of solar cells with surface macrostructure showed superior light absorption over our commercial solar cells with solar cells having the same p-n junction depth. Four hundred silicon wafers with 90 millimeter diameters can be diffused in one hour with a 38 inch flat zone furnace. The optimum low-cost, high energy-per-unit-area solar cell module can be determined by using modified hexagonal solar cells for maximum economy or by using full hexagonal solar cells for maximum power.

RECOMMENDATIONS

The work done in this study recommends the following: For maximum economy in the production of low-cost, high energy-per-unit-area solar cell modules one should utilize the modified hexagonal solar cells. For maximum solar cell module power one should utilize the full hexagonal solar cells.

NEW TECHNOLOGY

No new technology has been developed to completion for this quarterly report.

PROGRESS SUMMARY AND PROGRAM PLAN

The progress summary and program plan for Phase I and Phase II of the development of low-cost, high energy-per-unit-area solar cell modules is shown in Figure 17.

The program for the next quarter is outlined as follows:

1) A baseline cost analysis for Phase I will be done and a comparison will be made with cost estimates in Phase II.
2) Quantronix Corporation will complete and deliver to Sensor Technology the laserscribe computer program.
3) Surface macrostructure process studies will be completed and used on the solar cells for the Phase II modules.
4) Detailed diffusion studies will be completed comparing diffusion process types relative to solar cell production processes.
5) Phase I solar cell modules will be completed and delivered to JPL.
6) As requested by JPL spin-on equipment with production orientation will be procurred.

7) Spin-on studies will be conducted on anti-reflection coatings, dopants and photo-resists.

8) Phase II solar cell modules will be constructed.

Figure 17. Development of Low-Cost; High Energy-Per-Unit-Area Solar Cell Modules; Phase I and Phase II Program Plan

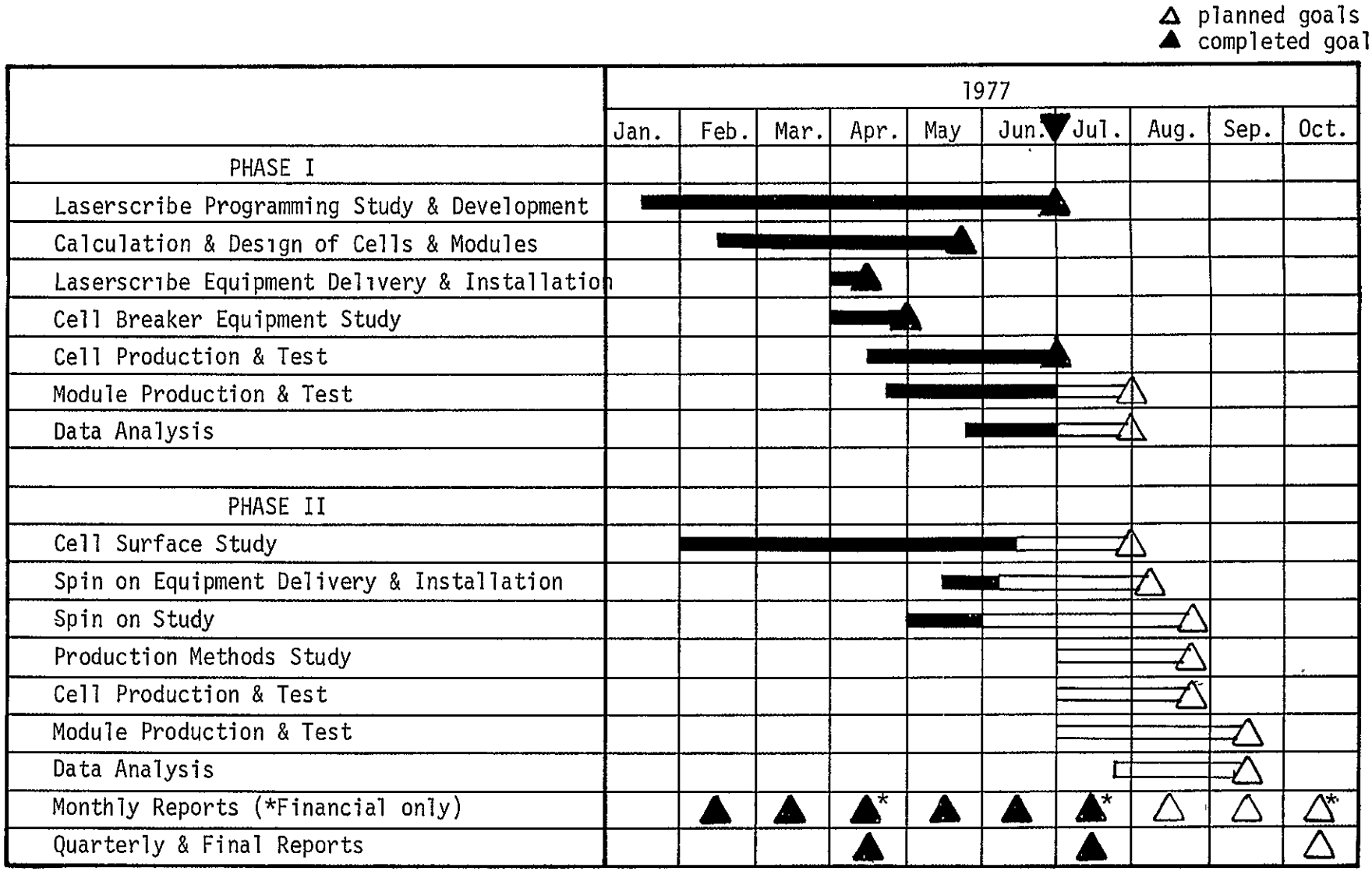

APPENDIX

A. Calculation of the Optimum Silicon Utilization in Modified Hexagonal Solar Cells

1. Boundary Conditions

Consider a hexagon with unit radius, an inscribed circle with radius equal to .866, and a circumscribed circle with unit radius. For a hexagon with fixed unit radius the silicon ingot radius can increase from .866 to 1.000. A silicon wafer with radius of .866 would be a circular wafer. A silicon wafer with radius equal to unity would have six sides cut forming a full hexagon. A silicon radius between .866 and 1.000 would form a modified hexagon.

Area of Hexagon with Unit Radius

$$A_H = 6\ (.500)\ (\cos 30^0) = 2.598$$

Area of Circumscribed Circle with Unit Radius

$$A_{CC} = \pi\ (1)^2 = 3.1416$$

Area of Inscribed Circle with .866 radius

$$A_{IC} = \pi\ (.866)^2 = 2.356$$

Silicon Fractional Utilization

Maximum, radius = .866, 100% utilized

Minimum, radius =1.000, full hexagon

A_H / A_{CC} = 82.7% utilized

Hexagon Fractional Utilization

Maximum, radius = 1.000, 100% utilized

Minimum, radius = .866, circular wafer

A_{IC} / A_H = 90.7% utilized

Boundary Conditions

Radius = .866, 100% silicon utilized, 90.7% hexagon utilized

Radius = 1.000, 82.7% silicon utilized, 100% hexagon utilized

2. Fractional Utilization of Silicon

For a given radius between .866 and 1.000, the fractional utilization of silicon material area to a circular silicon wafer area will now be calculated. The following calculations refer to Figure 18.

Area of (t x u)

Area (t x u) = Area (s x u) - Area (s t u)

Area (s x u) = $\frac{1}{2}$ (ux) R^2

where ux = $\frac{1}{2}$ (θ) (π/180) = .00873 θ (in radians)

Area (s t u) = $\frac{1}{2}$ (ut) (.866)

where ut = R sin (θ/2)

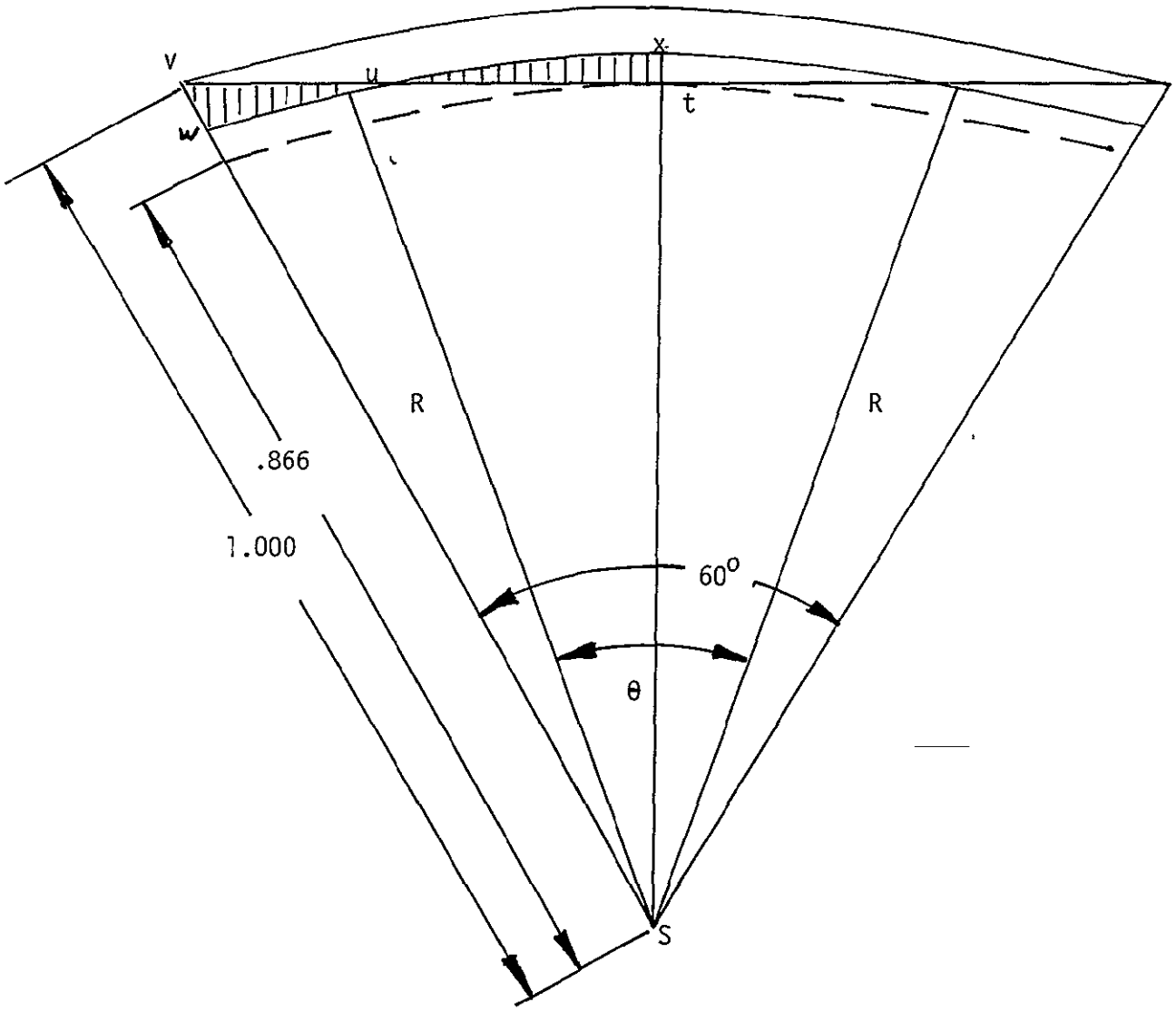

$.866 \leq R \leq 1.000$
$st = R \cos_1 \Theta/2 = .866$
$\theta = 2 \cos^{-1} (.866/R)$
$ut = R \sin (\theta/2)$
$vt = .500$

Figure 18. Section of modified hexagon illustrating silicon area (t x u) loss and hexagon area (u v w) loss.

Fractional Loss of Silicon

$$\text{Loss} = 12 \text{ (area } (t \times u)) / \pi R^2$$

Fractional Utilization of Silicon

$$\text{Utilization} = 1.000 - \text{Loss}$$

Table 1 lists the calculated results for determining the fractional utilization of silicon. Figure 13 gives a curve that shows the fractional utilization of silicon at unit cost.

3. Fractional Utilization of the Modified Hexagon

For a given radius between .866 and 1.000, the fractional utilization of the modified hexagon area to the full hexagon area will now be calculated. The following calculations refer to Figure 17.

Area of (u v w)

$$\text{Area (u v w)} = \text{area (s u v)} - \text{area (s u w)}$$

$$\text{Area (s u v)} = \text{area (s t v)} - \text{area (s t u)}$$

where area (s t v) = $\frac{1}{2}$ (.500) (.866) = .2165

and area (s t u) = $\frac{1}{2}$ (u t) (.866) = $\frac{1}{2}$ (R sin ($\theta/_2$)) .866

$$\text{area (s u w)} = \frac{1}{2} \text{ (u w) } R^2$$

where u w = $(30^0 - \theta/_2)$ $(\pi/180) = .01745\ (30^0 - \theta/_2)$

R	θ	Area (s x u)	Area (s t u)	Area (t x u)	12 (area (t x u))	Fractional Loss	Fractional Utilization
.866	0	0	0	0	0	0	1.000
.880	20.468	.0692	.0677	.0015	.0180	.0074	.993
.920	39.456	.1458	.1345	.0113	.1356	.0510	.949
.960	51.133	.2053	.1794	.0259	.3108	.1073	.893
.980	55.823	.2340	.1986	.0354	.4244	.1407	.859
1.000	60.000	.2619	.2165	.0454	.5448	.1734	.827

Table 1. Calculated results for determining the fractional utilization of silicon.

Fractional Loss of the Modified Hexagon

$$\text{Loss} = 12 \, (\text{area} \, (u \, v \, w)) \, / \, A_H$$

Fractional Utilization of Modified Hexagon

$$\text{Utilization} = 1.000 - \text{Loss}$$

Table 2 lists the calculated results for determining the fractional utilization of the modified hexagon. Figure 13 gives a curve that shows the fractional utilization of the modified hexagon at unit cost.

R	θ	Area (s t v)	Area (s t u)	Area (s u v)	Area (s u w)	Area (u v w)	12(area(uvw))	Fractional Loss	Fractional Utilization
.866	0	.2165	0	.2165	.1963	.0202	.2424	.0933	.907
.880	20.468	.2165	.0677	.1488	.1336	.0152	.0824	.0702	.930
.920	39.456	.2165	.1345	.0820	.0759	.0061	.0732	.0282	.972
.960	51.133	.2165	.1794	.0371	.0348	.0023	.0276	.0106	.989
.980	55.823	.2165	--	--	--	--	--	--	--
1.000	60.000	.2165	.2165	0	0	0	0	0	1.000

Table 2. Calculated results for determining the fractional utilization of the modified hexagon.

4. Incremental Cost Analysis

An incremental cost analysis of the silicon can be made by weighting the silicon unit cost curve given in Figure 13 and evaluating the results. The weighted cost calculations are shown as follows:

Weighted Cost

The weighted cost is given by

Cost = 1.000 - WF (Loss)

where WF is the weighting factor, i.i. ¼, ½, 1, 1½, 2, 3, and Loss is the fractional loss of silicon equal to 1.000 - fractional utilization of silicon. The results of these calculations are given in Table 3.

R	Utilized (Unit Cost)	Loss (Unit Cost)	¼ cost	½ cost	1½ cost	2 cost	3 cost
.866	1.000	0	1.000	1.000	1.000	1.000	1.000
.880	.993	.0074	.998	.996	.989	.985	.978
.920	.949	.0510	.987	.974	.924	.898	.847
.960	.893	.1073	.973	.946	.839	.785	.678
.980	.859	.1407	.964	.930	.789	.719	.578
1.000	.827	.1734	.957	.913	.740	.653	.480

Table 3. Calculated results for determining the fractional utilization of silicon for various costs, i.e. ¼, ½, 1, 1½, 2, 3 times the unit cost of silicon.

Incremental Cost

The incremental cost is the sum of the silicon material cost thrown away (silicon loss costs) plus the solar cell packaging costs (hexagon loss costs).

Example

Given a radius of .880 at 2 times unit silicon cost

Cost = .0702 + (1.000 - .985) = .085

Table 4 lists the calculated result which are plotted in Figure 14as silicon plus packaging incremental costs versus the cost radii for a cylinderical silicon ingot.

Radius / Cost Ratio	.866	.880	.920	.960	1.000	Minimum Cost Radius
3	.093	.092	.181	.333	.520	.874
2	.093	.085	.130	.226	.347	.880
1½	.093	.081	.104	.172	.260	.886
1	.093	.077	.079	.118	.173	.896
½	.093	.074	.054	.065	.087	.920
¼	.093	.072	.041	.038	.043	.948

Table 4. Calculated results for determining the incremental cost of the silicon material thrown away plus the solar cell packaging for normalized silicon ingot radii between .866 and 1.00. Included is the minimum cost radii read from the curves in Figure 15.

Minimum Incremental Cost

The minimum incremental cost is read off the curves in Figure 14 and are plotted for the silicon cost to packaging cost ratio versus the normalized silicon ingot radius in Figure 15. Figure 15 is very useful in determining the optimum silicon utilization in modified solar cells and to produce the optimum solar cell module system.

APPENDIX

B. LIST OF DEFINITIONS

The following terms are defined as used in reports on this development program:

Modified Hexagon - the figure resulting when a hexagon is cut from a circle with a diameter smaller than the point to point diameter of the hexagon.

Scribe - to partially cut by laser into a silicon wafer in preparation for breaking.

Laserscribe - a machine which has a focused laser beam and a computer for controlling the position and velocity of a moveable platform carrying the silicon wafer for scribing.

Surface Macrostructure - the surface structure resulting from differential etching along the silicon crystal planes, so that radiant energy will be absorbed more efficiently.

Solar Cell Packing Ratio - the sum of the solar cell surface areas divided by the area of the solar cell module.

Solar Cell Nesting Area - the module surface area that contains the solar cells which includes the total solar cell surface area plus the solar cell spacing area.

Solar Cell Packaging Material - the substrate material and encapsulant material required by the solar cell nesting area.

Module Border Packaging Material - the substrate material and encapsulation material required by the module border. It includes the module edges and terminal connection areas.

Solar Cell Module Packaging Material - the module substrate material, encapsulation material, and terminals with terminal connections.

Solar Cell Modules - the module substrate, encapsulation material, terminals with terminal connections, solar cells and solar cell interconnects.

Solar Cell Module Systems - the solar cell module, mounting frame, module interconnections and land areas.

Solar Cell Packaging Costs - the material and labor costs for the module substrate and encapsulant required by the solar cell nesting area.

Module Border Packaging Costs - the material and labor costs for the module substrate and encapsulation required by the module border. It includes the cost of the module edges and terminal connection areas.

Solar Cell Module Packaging Costs - the material and labor costs for the module substrate, encapsulation, terminals and terminal connections, solar cells and solar cell interconnects.

Solar Cell Module System Costs - the material and labor costs for the solar cell modules, mounting frame, module interconnections, and land area. It includes all fees and general expenses incurred in constructing the system.